Limiting Factors in Tropospheric Propagation Delay Error Modelling for GPS Airborne Navigation‡

Paul Collins and Richard Langley
Geodetic Research Laboratory, Department of Geodesy and Geomatics Engineering, University of New Brunswick, Canada.

James LaMance
NAVSYS Corporation, Colorado Springs, CO, U.S.A.

BIOGRAPHIES

Paul Collins graduated from the University of East London in 1993 with a B.Sc. (Hons) in Surveying and Mapping Sciences. He is currently enrolled in the M.Sc.E. degree program in the Department of Geodesy and Geomatics Engineering at UNB, where he is investigating the effect of the troposphere on kinematic GPS positioning.

Richard Langley is a professor in the Department of Geodesy and Geomatics Engineering at the UNB, where he has been teaching since 1981. He has a B.Sc. in applied physics from the University of Waterloo and a Ph.D. in experimental space science from York University, Toronto. Dr. Langley has worked extensively with GPS. He is a co-author of the best-selling *Guide to GPS Positioning* published by Canadian GPS Associates and is a columnist for *GPS World* magazine. He has helped develop and present a number of seminar courses on GPS for both Canadian GPS Associates and the American-based Navtech Seminars Inc. Dr. Langley has consulted extensively in the field of GPS with private companies and government agencies both in Canada and abroad.

James LaMance is a Senior Engineer at NAVSYS Corporation, in Colorado Springs, CO, where he is involved with GPS navigation systems design and analysis. Dr. LaMance has worked in the areas of GPS, remote sensing and orbit determination for the past seven years. Dr. LaMance holds a Ph.D. and M.S. in Aerospace Engineering from the University of Colorado at Boulder, and a B.S. in Aerospace Engineering from Auburn University.

ABSTRACT

We examine the likely accuracies to which the tropospheric propagation delay at the zenith can be modelled in airborne navigation and the limiting effects this will ultimately have on an aircraft's position determination. Even though the hydrostatic component of the tropospheric zenith delay can be modelled to millimetre accuracy, this requires an accurate atmospheric pressure measurement. In aircraft navigation this may not be directly available and the pressure value used to drive the model must be derived from another source. Whatever average value is used, it is unlikely to represent the real pressure exactly and will therefore introduce a bias into the delay determination.

To observe the effects of the neutral atmosphere on GPS signals, dual frequency (L1 and L2) GPS data was collected with Ashtech Z-12 receivers at a surveyed base station and simulataneously on board an aircraft. Kinematic position solutions for the aircraft have been computed from the data sets. The effects of the troposphere have been examined by looking at differences in position solutions using different tropospheric delay models.

Our results indicate that the water vapour component of the tropospheric delay provides the limiting factor close to the earth's surface. If the value used for water vapour pressure is incorrect compared to the "true" value by the order of 10 mbar, then in the absence of other errors, the resulting zenith delay will be in error by the order of 10 cm Towards the tropopause however, incorrect scaling of the total surface pressure provides the limiting factor.

‡ Presented at The Institute of Navigation 52nd Annual Meeting, Cambridge, Massachusetts, USA, 19th - 21st June, 1996

INTRODUCTION

It has been shown previously [*Mendes et al.*, 1995, *Collins and Langley*, 1996] that the methods of modelling the tropospheric delay for geodetic-type static GPS positioning can be applied to navigation purposes provided that suitable meteorological parameters are specified to drive the models. Suitable in this context means surface values that are as close to actual values as possible and importantly, the correct method of scaling them to the user's altitude. Hence the problem becomes one of adequately modelling the real atmosphere at any particular time and place.

The impetus for our research has been the requirement for a tropospheric delay model for the Federal Aviation Administration's (FAA) Wide Area Augmentation System (WAAS) for civilian aircraft navigation using GPS. In this paper we concentrate on presenting improved methods of modelling the troposphere and on the development of an error model for the tropospheric delay.

TROPOSPHERIC DELAY

The propagation delay of the GPS signal caused by the non-ionised, or neutral atmosphere (usually referred to as the tropospheric delay), can be considered as the combined effect of the delay experienced at the zenith and the ratio of that delay to the delay at the elevation angle of the raypath. These ratios are usually termed mapping functions. Following *Davis et al.* [1985], the typical formulation of the tropospheric delay is given as:

$$d_{trop} = d^z_{hyd} \cdot m_{hyd} + d^z_{wet} \cdot m_{wet}\,, \qquad (1)$$

where the total delay d_{trop} is a function of the hydrostatic zenith delay d^z_{hyd} and its mapping function m_{hyd} and the wet zenith delay d^z_{wet} and its mapping function m_{wet}.

The zenith delay components d^z_{hyd} and d^z_{wet} are functions of the total atmospheric pressure (P in mbar), and temperature (T in kelvins) and water vapour pressure (e in mbar) respectively. Values that represent these parameters must be supplied by the user to indicate the ambient conditions at the GPS antenna. As such, the delays can be approximated by:

$$d^z_{hyd} = \tau^z_{hyd} \cdot P \quad , \qquad (2)$$

and

$$d^z_{wet} = \tau^z_{wet} \cdot \frac{e}{T} \quad , \qquad (3)$$

respectively, where τ^z_{hyd} and τ^z_{wet} represent the models to compute the path delays from the ambient meteorological parameter values.

TROPOSPHERIC DELAY MODELS

We are using the combination of the Saastamoinen zenith delays and Niell mapping functions as a basis for our work. The Saastamoinen hydrostatic zenith delay per millibar of ambient pressure is in the form presented by *Davis et al.*, [1985]:

$$\tau^z_{hyd} = \frac{10^{-6} k_1 R}{g_m} \quad , \qquad (4)$$

and the wet zenith delay per millibar of ambient water vapour pressure and per inverse kelvins is the explicit formulation outlined by *Askne and Nordius* [1987] which includes the temperature lapse rate (β in K/km) and water vapour "lapse rate" (λ, see next section):

$$\tau^z_{wet} = \frac{10^{-6}\left(T_m k'_2 + k_3\right)R}{g_m \lambda' - \beta R} \quad , \qquad (5)$$

where the mean temperature of the water vapour $T_m = T\left(1 - \frac{\beta R}{g_m \lambda'}\right)$, g_m represents the gravity acceleration at the atmospheric column centroid, $\lambda' = \lambda + 1$ and is unitless, R is the gas constant for dry air and k_1, k'_2 and k_3 are refractivity constants (see e.g. *Thayer* [1974]).

The Niell mapping functions [*Niell*, 1966] are parameterised in terms of positional information (latitude and height) and time (day-of-year) only. They require no user input of meteorological information yet have been shown to work as well as, if not better than other mapping functions that do (see e.g. *Mendes and Langley* [1994]). They are derived from ray-traces of the 1966 U.S. Standard Atmosphere Supplements [ESSA/NASA/USAF, 1966] which provide climatic data for 15°, 30°, 45°, 60° and 75° latitudes for the January and July extremes of winter and summer conditions in the northern hemisphere. The southern hemisphere is assumed anti-symmetric in time.

TROPOSPHERE MODELS

The simplest method of modelling the atmosphere is to provide surface parameters coupled with expressions to describe the change with height through the atmosphere. As the primary driving parameters of the tropospheric delay it is natural that we choose total pressure (P_0), temperature (T_0) and water vapour pressure (e_0) at the surface. The vertical profile of these parameters can be specified through the temperature lapse rate (β) and a parameter that represents the average decrease of water vapour (λ) [*Smith*, 1966].

The temperature lapse rate is assumed linear with height (H):

$$T = T_0 - \beta \cdot H \quad , \tag{6}$$

which, coupled with the condition of hydrostatic equilibrium and application of the perfect gas law, yields the standard expression:

$$P = P_0 \left(\frac{T}{T_0} \right)^{\frac{g}{R\beta}} \quad . \tag{7}$$

The average decrease in water vapour is assumed to be described by the power law (see e.g. *Askne and Nordius* [1987]):

$$e = e_0 \left(\frac{P}{P_0} \right)^{\lambda'} \tag{8}$$

and hence:

$$e = e_0 \left(\frac{T}{T_0} \right)^{\frac{\lambda' g}{R\beta}} \quad , \tag{9}$$

where surface gravity is represented by *g*. From these equations we can derive the following expressions to scale the surface values to the user's height:

$$\begin{aligned} P &= P_0 \left(1 - \frac{\beta H}{T_0} \right)^{\frac{g}{R\beta}} \quad , \\ &\equiv P_0 \cdot \kappa_{hyd}\left(T_0, \beta\right) \end{aligned} \tag{10}$$

$$\begin{aligned} \frac{e}{T} &= \frac{e_0}{T_0} \left(1 - \frac{\beta H}{T_0} \right)^{\frac{\lambda' g}{R\beta} - 1} \quad . \\ &\equiv \frac{e_0}{T_0} \cdot \kappa_{wet}\left(T_0, \beta, \lambda'\right) \end{aligned} \tag{11}$$

Combining equations (10) and (11) with (2) and (3) allows us to formulate the zenith delays as follows:

$$d^z_{hyd} = \tau^z_{hyd} \cdot \kappa_{hyd} \cdot P_0 \quad , \tag{12}$$

$$d^z_{wet} = \tau^z_{wet} \cdot \kappa_{wet} \cdot \frac{e_0}{T_0} \quad . \tag{13}$$

Specifically for the airborne environment, we can see that the hydrostatic delay is dependent upon the surface pressure and the temperature profile. The wet delay is dependent upon both the temperature profile and the water vapour profile. This formulation is particularly useful for deriving an error model for the tropospheric delay.

All the models represented here are limited to use below the tropopause. In isothermic layers the scaling functions κ_{hyd} and κ_{wet} are not valid and must be replaced. They then become a function of the pressure at the base of the isothermic layer.

These five meteorological parameters of pressure, temperature, and partial pressure of water vapour at the surface, coupled with the temperature lapse rate and water vapour "lapse rate" provide a simple, yet comprehensive method for modelling the neutral atmosphere. Of course no matter how well we represent the mean structure of the atmosphere there can at any one time be a significant variation.

Our previous tropospheric delay model [*Collins and Langley*, 1996] used the Saastamoinen models driven by a set of constant values to represent the mean global atmosphere. These values represent the standard surface values for temperature and pressure with a value for water vapour pressure derived to be equivalent to the mean global surface refractivity of 324.8 N units. The temperature lapse rate is considered to be the global average, as is the value for lambda [*Saastamoinen*, 1973]. This model was designated UNB1 and its parameters are given in Table 1.

Table 1. Parameters for UNB1 model. (See text for associated units).

P_0	T_0	e_0	β	λ
1013.25	288.15	11.691	6.5	3

Due to the stochastic nature of water vapour, the lambda parameter is only ever representative of the average decrease in water vapour in a column of air.

Even if it is derived from real-time measurements it is then only accurate for those space and time scales over which it was derived (see e.g. *Schwarz* [1968] and *Smith* [1968]). However, the water vapour profile does exhibit a latitudinal trend over the atmosphere as a whole and zenith delay models with constant values for lambda have been shown to perform poorly at high latitudes (see e.g. *Ifadis* [1986]).

A similar latitudinal (or zonal) variation is true of the atmosphere as a whole, hence it was apparent that an attempt should be made to provide average annual latitudinal values of the five parameters. Surface pressure values are provided in *Trenberth* [1981]; the global temperature structure is given in *Fleming et al*. [1988], from which average zonal surface temperature and lapse rates can be derived; and *Peixoto and Oort* [1983] provide data from which surface water vapour and its lapse rate can be derived. The parameter values of such a model are listed in Table 2; the model has been designated UNB2.

Table 2. Parameters for UNB2 model. (See text for associated units).

Lat	P_0	T_0	e_0	β	λ
80	1015.0	259.8	2.6	3.88	2.24
70	1013.1	266.1	4.0	4.49	2.55
60	1012.4	274.9	6.4	5.31	2.96
50	1014.5	281.8	9.2	5.86	3.18
40	1016.6	288.7	13.8	6.20	3.52
30	1016.1	294.8	19.6	6.23	3.42
20	1013.2	298.7	25.1	6.18	3.29
10	1010.7	300.5	28.6	6.18	3.33
0	1010.3	300.5	28.3	6.16	3.21
-10	1011.6	300.0	26.7	6.14	3.23
-20	1014.8	297.6	22.3	6.10	3.41
-30	1017.7	293.5	17.4	6.20	3.30
-40	1014.8	287.6	12.4	6.19	3.46
-50	1003.2	280.4	8.2	5.91	3.22
-60	988.5	274.9	5.3	5.71	3.00
-70	987.5	271.0	3.5	5.57	3.45

As will be seen later, this model represents an improvement over UNB1, however its make up is rather *ad hoc* and its coverage only extends from 80°N to 70°S because of the incomplete coverage of some of the data from which it was derived. At the same time it was thought that an improvement might be gained by introducing a temporal variation. It was therefore decided to apply the concepts used by the Niell mapping functions to a troposphere model. These functions represent the annual variation of the atmosphere as a sinusoidal function of the day-of-year. Given the proven performance of the Niell mapping functions, it was thought that a troposphere model derived from the same data would be useful.

To this end, the temperature and humidity profiles contained in the 1966 U.S. Standard Atmosphere Supplements were used to derive values for the five meteorological parameters. For each latitude in the standard, the mean and the amplitude of the five parameters were calculated from the January and June profiles. Between latitudes, linear interpolation is applied so that for a required parameter ξ at latitude ϕ and time t:

$$\xi(\phi,t) = \xi_{avg}(\phi_i) + \left[\xi_{avg}(\phi_{i+1}) - \xi_{avg}(\phi_i)\right]\cdot m - \left(\xi_{amp}(\phi_i) + \left[\xi_{amp}(\phi_{i+1}) - \xi_{amp}(\phi_i)\right]\cdot m\right) \cdot \cos\left(\frac{2\pi(t-28)}{365.25}\right) \quad (14)$$

where $m = (\phi - \phi_i)/(\phi_{i+1} - \phi_i)$. The subscripts refer to the nearest latitudes specified in the table to the required one. For consistency with the Niell functions, day-of-year 28 is used for the phase of the temporal variation. This model is described in Table 3 and is designated UNB3.

Table 3. Parameters for UNB3 model. (See text for associated units).

Mean	P_0	T_0	e_0	β	λ
15	1013.25	299.65	26.31	6.30	2.77
30	1017.25	294.15	21.79	6.05	3.15
45	1015.75	283.15	11.66	5.58	2.57
60	1011.75	272.15	6.78	5.39	1.81
75	1013.00	263.65	4.11	4.53	1.55
Amp.	P_0	T_0	e_0	β	λ
15	0.00	0.00	0.00	0.00	0.00
30	-3.75	7.00	8.85	0.25	0.33
45	-2.25	11.00	7.24	0.32	0.46
60	-1.75	15.00	5.36	0.81	0.74
75	-0.50	14.50	3.39	0.62	0.30

NON-RANDOM ERROR MODELLING

For our error model we wish to study the potential impact on the tropospheric delays caused by potential deviations of the "real" atmosphere from the model atmosphere. The error propagation model developed is a direct application of the propagation of error law. The partial derivatives of the zenith delay functions and the scaling functions are taken with respect to the surface

meteorological parameters and the lapse rates. All non-atmospheric parameters are treated as stochastic and uncorrelated to represent the inherent uncertainties in the models. When dealing with the atmospheric parameters, it must be realised that at any one time these will be biased compared to the "true" values. Hence the atmospheric parameters are propagated as biases and not as random errors (cf. *Beutler et al.* [1987]). This approach has been verified by comparing the error model against differences in zenith delays computed using model parameters and simulated biases.

For the correct application of the error propagation law, the magnitude of the error should be small so that the linear approximation of Taylor's expansion can be used. Unfortunately the lapse rate parameters β and λ are subject to large variations that violate this condition. Therefore it is likely that the error model itself is only accurate at the centimetre level. At the same time it must also be borne in mind that this model represents the formal errors of the tropospheric delay models. It can be difficult to satisfactorily apply the model in considering errors induced by the "real" atmosphere, due to the potential for inversion layers and other anomalies, however the general impact of each of the components of the tropospheric model on the determination of the tropospheric delay can be assessed.

For example, if we assume that UNB3 better represents the real atmosphere for January at 75 degrees latitude then we can examine how the differences in the tropospheric parameters from those specified in UNB1 affect the zenith delay determination. Figure 1 illustrates the impact of these variations on the components of the hydrostatic zenith delay as described by the error model. (Note: the delay error is the residual delay that would have to be added to the UNB1 model to obtain the "correct" delay).

Obviously the slight difference in surface pressure does not have much impact, but the variation in the temperature profile does. The combination of biases in the surface temperature and lapse rate can introduce a significant bias into the delay determination as the users height increases. Considering the formulation of the hydrostatic zenith delay (eq. 12), we can conclude that this is entirely due to the influence of the scaling factor κ_{hyd} (eq. 10).

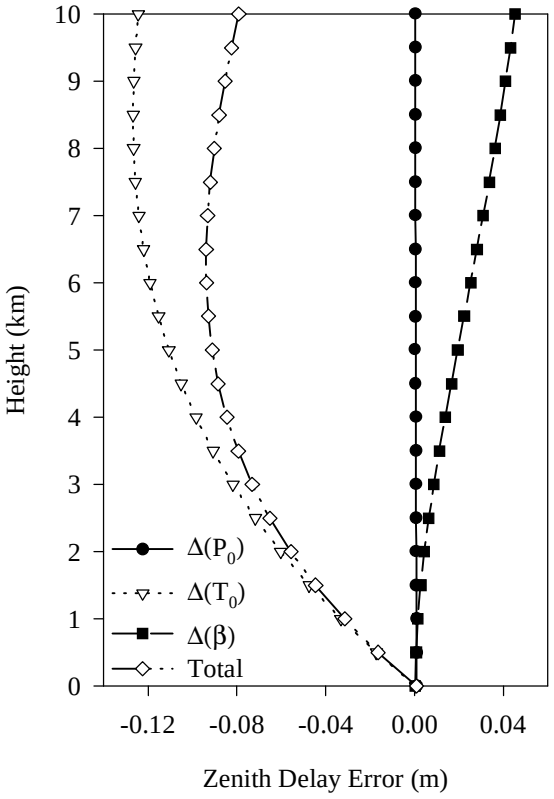

Figure 1. Hydrostatic zenith delay error (total and separate components) between UNB1 and UNB3 for January at 75°N latitude [ΔP_0 = +0.25 mbar, ΔT_0 = -38.9 K, $\Delta\beta$ = -2.6 K/km].

In comparison, the impact of the same variation of the temperature profile on the wet delay d^z_{wet} is small. Figure 2 shows the error model applied to the zenith wet delay for the differences between UNB3 and UNB1 for January at 75 degrees latitude. Here we see the greatest effect coming from variations in the water vapour profile. The changes in temperature profile generally affect the zenith wet delay by approximately 1 cm or less. The modelling of the wet zenith delay error is more complex due to the fact that the temperature and water vapour lapse rates appear in both the delay function τ^z_{wet} and the scaling function κ_{wet}. The lambda parameter has the greater effect as Figure 2 shows and in general the bias introduced by an uncertain lambda value depends directly on the amount of surface water vapour pressure and vice versa.

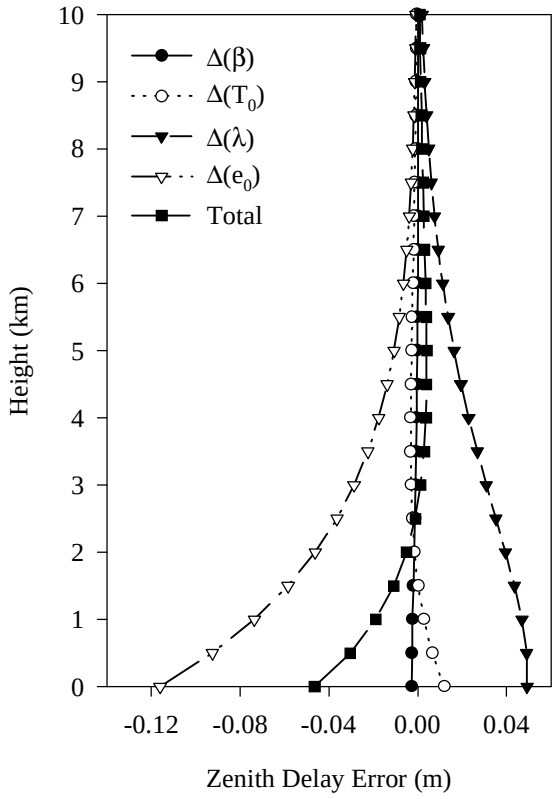

Figure 2. Wet zenith delay error (total and separate components) [Δe_0 = -10.98 mbar, ΔT_0 = -38.9 K, $\Delta\beta$ = -2.6 K/km, $\Delta\lambda$ = -1.75].

Overall, the bias in the wet zenith delay is much larger at the surface than the hydrostatic delay. The total zenith delay bias is the sum of the hydrostatic and wet biases. It is obviously possible for these to cancel out at certain times. However the rapid decrease of water vapour usually means that the hydrostatic bias is dominant above the first few kilometres.

CONSIDERATIONS ON ERROR MODELLING

What becomes obvious is that to improve a model's overall performance - that is to keep a certain consistency at all heights - the temperature profile must be considered slightly differently than we have previously. The existence of any temperature inversion in the atmospheric boundary layer will degrade the accuracy of the hydrostatic scaling factor κ_{hyd}. Because its impact on the wet delay is comparatively small, a "surface" temperature can be extrapolated down from the tropopause. It is largely accepted that, above the boundary layer, the lapse rate has a minimal variation across all latitudes (*Smith* [1963]), therefore at the same time we can choose to use a constant lapse rate of 6.5 K/km. These changes have been applied to UNB3 to arrive at UNB4 (see Table 4).

Table 4. Parameters for UNB4 model.

Mean	P_0	T_0	e_0	β	λ
15	1013.25	301.70	26.31	6.50	2.77
30	1017.25	298.65	21.79	6.50	3.15
45	1015.75	292.40	11.66	6.50	2.57
60	1011.75	281.35	6.78	6.50	1.81
75	1013.00	278.90	4.11	6.50	1.55
Amp.	P_0	T_0	e_0	β	λ
15	0.00	0.00	0.00	0.00	0.00
30	-3.75	4.50	8.85	0.00	0.33
45	-2.25	7.75	7.24	0.00	0.46
60	-1.75	8.80	5.36	0.00	0.74
75	-0.50	9.00	3.39	0.00	0.30

In this way the greatest difference between UNB3 and UNB4 in surface temperature is for the January 75° Atmosphere. The difference is approximately 20 K, however the water vapour pressure is so low that the lambda parameter has the greatest impact on the wet delay error. The actual differences for the wet zenith delay between the two models is approximately one millimetre with an inherent uncertainty of $\lambda' = 2.25 \pm 1$ contributing a potential bias of approximately 6 mm in the zenith delay for these conditions.

For the sake of computational efficiency and simplicity it is possible to simplify the wet zenith delay expression (eq. 5) a little. Again following *Davis et al*. [1985], the refractivity constants can be combined by specifying a global value for the mean temperature (T_m). Choosing 260 ± 20 K we can derive $k'_3 = T_m k'_2 + k_3 = (3.82 \pm 0.04) \times 10^5$ K^2/mbar. This approximation accounts for a difference of less than 1 millimetre of zenith wet delay under most conditions.

DATA PROCESSING AND RESULTS

We are continuing to use the flight data collected by the National Research Council of Canada, at and around St. John's, Newfoundland, in March 1995. The dual frequency GPS data for twelve flights collected at a reference station near the airport and onboard an aircraft is processed with simultaneously recorded meteorological data to provide a reference or "benchmark" solution. The solution is then re-computed using the candidate tropospheric model to compute the tropospheric delay at the aircraft. With this method we can assess the impact on the aircraft's position of a change in the tropospheric delay model.

Table 5 represents a statistical evaluation of the performance of the models we have developed so far. Both average and maximum values for the maximum difference, the bias, standard deviation and root mean square (rms) error between the benchmark solution and a particular solution are provided. From this table alone it would appear that UNB3 performs poorly compared to UNB2. Looking at the height component, the standard deviations are similar, but the bias is much greater.

Unfortunately these statistics alone do not represent the true performance of each model. An inspection of model performance with height reveals why. As an example, consider Figure 3. This figure represents the differences from the benchmark solution in the height component for the flight of March 15th. As can be seen, the UNB3 model has removed the trend at low altitudes only to introduce one at higher altitudes. By only considering the results below a height of 500 metres, we perceive a slightly different overall picture - see Table 6.

From Table 6 we can see the improved performance of UNB3 at low altitudes. The standard deviation of the solution differences is the same (~5 cm), however the bias is much lower. As can clearly be seen from Figure 4a, which represents the temperature profile recorded during this flight, UNB3 represents more closely the temperature profile at low altitudes, however because of the temperature inversions it is less accurate above the boundary layer. Figure 4b indicates the reason for the improved performance of UNB3 and UNB4 at low altitudes – that is their more accurate representation of the water vapour profile as recorded at the aircraft.

Table 5. Average (mean) and worst case (max) values of maximum difference, bias, standard deviation and root-mean-square statistics for all solutions computed using all the data.

		Latitude Difference (m)				Longitude Difference (m)				Height Difference (m)			
		max	bias	sd	rms	max	bias	sd	rms	max	bias	sd	rms
UNB1	mean	0.09	0.00	0.02	0.02	0.06	0.00	0.02	0.02	0.45	0.08	0.10	0.15
	max	0.15	0.02	0.04	0.04	0.10	0.01	0.02	0.03	0.71	0.20	0.16	0.26
UNB2	mean	0.07	0.00	0.02	0.02	0.05	0.00	0.01	0.01	0.35	0.01	0.09	0.11
	max	0.11	0.01	0.03	0.03	0.07	0.01	0.02	0.02	0.54	0.13	0.13	0.18
UNB3	mean	0.08	0.00	0.02	0.02	0.05	0.00	0.01	0.01	0.35	-0.06	0.10	0.13
	max	0.16	0.02	0.04	0.04	0.10	0.02	0.03	0.03	0.62	0.21	0.14	0.25
UNB4	mean	0.06	0.00	0.01	0.02	0.04	0.00	0.01	0.01	0.32	0.02	0.08	0.11
	max	0.10	0.01	0.02	0.03	0.08	0.01	0.02	0.02	0.50	0.12	0.11	0.15

Table 6. Average (mean) and worst case (max) values of maximum difference, bias, standard deviation and root-mean-square statistics for all solutions computed using data below 500 metres.

		Latitude Difference (m)				Longitude Difference (m)				Height Difference (m)			
		max	bias	sd	rms	max	bias	sd	rms	max	bias	sd	rms
UNB1	mean	0.08	0.00	0.03	0.03	0.05	-0.01	0.02	0.02	0.41	0.22	0.08	0.23
	max	0.15	0.05	0.05	0.06	0.10	0.02	0.03	0.04	0.71	0.40	0.14	0.42
UNB2	mean	0.05	0.00	0.02	0.02	0.03	0.00	0.01	0.02	0.27	0.13	0.05	0.14
	max	0.10	0.03	0.03	0.04	0.06	0.02	0.02	0.03	0.48	0.27	0.10	0.28
UNB3	mean	0.03	0.00	0.01	0.01	0.02	0.00	0.01	0.01	0.19	0.07	0.04	0.09
	max	0.07	0.02	0.02	0.03	0.05	0.01	0.02	0.02	0.39	0.22	0.09	0.23
UNB4	mean	0.03	0.00	0.01	0.01	0.02	0.00	0.01	0.01	0.20	0.08	0.05	0.10
	max	0.07	0.02	0.02	0.03	0.05	0.01	0.02	0.02	0.41	0.23	0.09	0.24

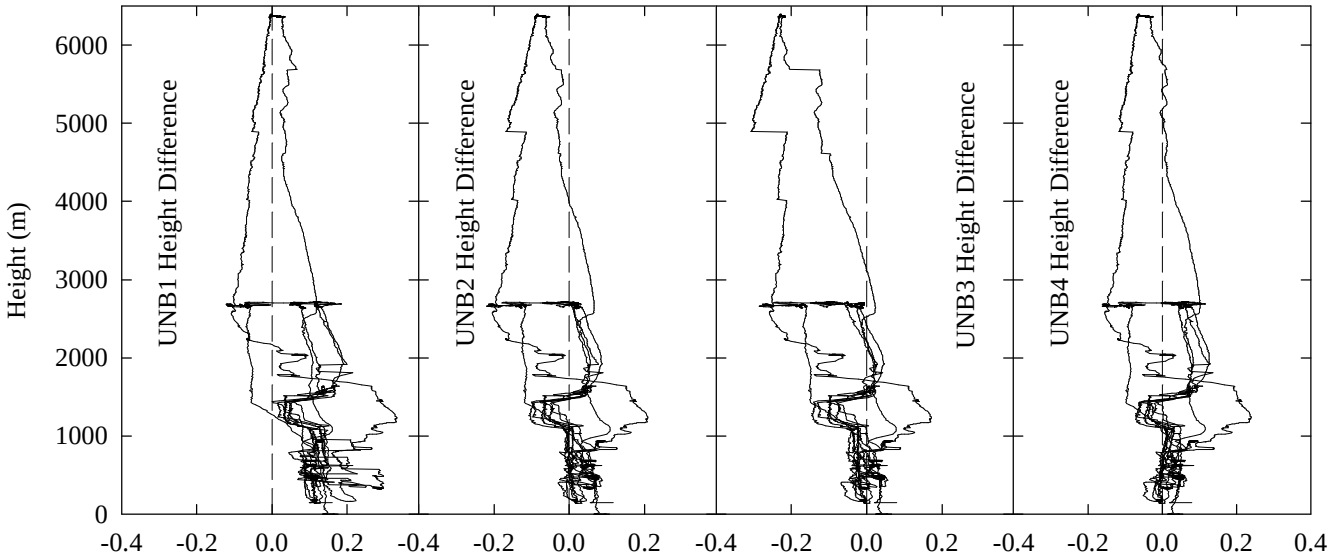

Figure 3. Solution differences for 15th March plotted against height of aircraft. All x-axis units are metres.

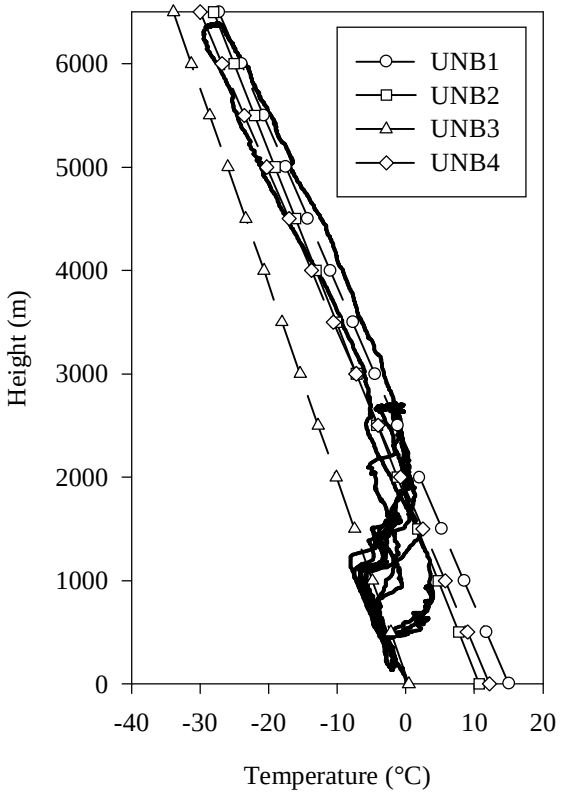

Figure 4a. Temperature profile recorded at aircraft for March 15th. Profiles for the UNB models at the reference station are superimposed.

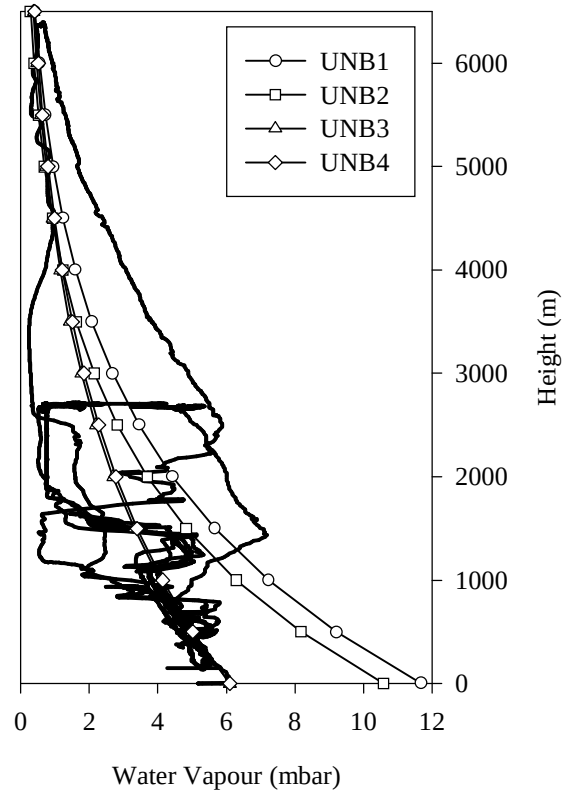

Figure 4b. Water vapour profile recorded at aircraft for March 15th. Profiles for the UNB models at reference the station are superimposed.

Considering the statistics pertaining to UNB4, they indicate that, taken over the whole flight path, the UNB4 model provides the best solution of the four models tested here. The values for the model's performance below 500 metres are approximately 1 cm larger than for UNB3. This difference is probably due to the difference in temperature profile between the two models and is almost certainly within the inherent uncertainty of the wet delay.

These statistics coupled with an examination of Figures 3 and 4 confirm the results of the error modelling from the previous section. That is, a significant variation in the temperature profile away from a single linear lapse rate indirectly introduces a bias into the tropospheric delay determination through the hydrostatic delay. This generally occurs above the first few kilometres above the surface where the bias in the wet delay is dominant.

CONCLUSIONS

Considering the small spatial and temporal extent represented by our data set, the 1966 Standard Atmosphere Supplements appear to represent the real atmosphere more closely than global average or latitudinal average parameters. From this data alone however, it is not possible to make any accurate assessment of the global or hemispheric performance of our models. For example, it is often assumed that the southern hemisphere is a mirror of the northern hemisphere. However, UNB2 shows that there are significant differences in the average total surface pressure in the southern hemisphere. Hence the provision of some kind of annual variation to that model may provide an improvement over UNB3.

While we are able in many cases to remove much of the bias previously seen at low altitudes between the benchmark solutions, large variations can still be seen within the solution differences. This is primarily due to the large variation of water vapour pressure and it is this that will likely provide the ultimate limiting factor in aircraft positioning. As we have seen with UNB3 and UNB4 however, it is possible to significantly improve the determination of the tropospheric delay near to the surface, for airborne navigation.

The error propagation model reinforces the fact that, provided care is taken with the adopted temperature profile, the potential tropospheric delay error increases to a maximum at the earth's surface. The unpredictability of the water vapour profile provides the greatest uncertainty as it does in other GPS positioning applications.

Future work will involve the testing of UNB3 and UNB4 with meteorological data sets more representative of differing climatic conditions. The error model will be extended and tested to provide the tropospheric range error contribution to pseudorange measurements.

ACKNOWLEDGEMENTS

The support of Transport Canada Aviation, the Natural Sciences and Engineering Research Council of Canada, the Atmospheric Environment Service and the Federal Aviation Administration are gratefully acknowledged.

REFERENCES

Askne, J. and H. Nordius (1987). "Estimation of tropospheric delay for microwaves from surface weather data." *Radio Science*, Vol. 22, No. 3, pp. 379-386.

Beutler, G., I. Bauersima, W. Gurtner, M. Rothacher, T. Schildknecht (1987). "Atmospheric refraction and other important biases in GPS carrier phase observations" in: *GPS Papers Presented by the Astronomical Institute of the University of Berne*, Ed. W. Gurtner, Miteilungen der Satellitenbeobachtungs-station Zimmerwald, Nr. 22, University of Berne, Switzerland, 26 pp.

Collins, J.P. and R.B. Langley (1996). "Mitigating Tropospheric Propagation Delay Errors in Precise Airborne GPS Navigation." *Proceedings of PLANS '96*, IEEE, Atlanta, GA, 22-26 April, pp. 582-589.

Davis, J.L., T.A. Herring, I.I. Shapiro, A.E.E. Rogers and G. Elgered (1985). "Geodesy by radio interferometry: Effects of atmospheric modelling errors on estimates of baseline length." *Radio Science*, Vol. 20, No. 6, pp. 1593-1607.

ESSA/NASA/USAF (1966). *U.S. Standard Atmosphere Supplements, 1966*. U.S. Committee on Extension to the Standard Atmosphere. U.S. Government Printing Office, Washington, DC.

Fleming, E.L., S. Chandra, M.R. Schoeberl and J.J. Barnet, (1988). *Monthly mean Global Climatology of Temperature, Wind, Geopotential Height and Pressure for 0-120 km*. NASA TM-100697. Goddard Space Flight Center, Greenbelt, MD.

Ifadis, I. (1986). *The atmospheric delay of radio waves: Modelling the elevation dependence on a global scale*. Technical Report 38L, Chalmers University of Technology, Goteborg, Sweden.

Mendes, V.B. and R.B. Langley (1994). "A comprehensive analysis of mapping functions used in modeling tropospheric propagation delay in space geodetic data." *Proceedings of KIS94, International Symposium on Kinematic Systems in Geodesy, Geomatics and Navigation*, Banff, Canada, 30 August - 2 September, pp. 87-98.

Mendes, V.B., J.P. Collins and R.B. Langley (1995). "The effect of tropospheric propagation delay errors in airborne GPS precise positioning." *Proceedings of ION GPS-95*, Palm Springs, CA, 12-15 September 1995, pp. 1681-1689.

Niell, A.E. (1996). "Global mapping functions for the atmosphere delay at radio wavelengths." *Journal of*

Geophysical Research, Vol. 101, No. B2, pp. 3227-3246.

Peixoto, J.P. and A.H. Oort (1983). "The atmospheric branch of the hydrological cycle and climate" in *Variations in the Global Water Budget*, D. Reidel, Hingham, MA, pp. 5-65.

Thayer, G.D. (1974). "An improved equation for the radio refractive index of air." *Radio Science*, Vol. 9, No. 10, pp. 803-807.

Trenberth, K.E. (1981). "Seasonal Variations in Global Sea Level Pressure and the Total Mass of the Atmosphere." *Journal of Geophysical Research*, Vol. 86, No. C6, pp. 5238-5246.

Saastamoinen, J. (1973). "Contributions to the theory of atmospheric refraction." In three parts: *Bulletin Géodésique*, No. 105, pp. 270-298; No. 106, pp. 383-397; No. 107, pp. 13-34.

Schwarz, F.K. (1968). "Comments on 'Note on the Relationship between Total Precipitable Water and Surface Dew Point'." *Journal of Applied Meteorology*, Vol. 7, pp. 509-510.

Smith, J.W. (1963). "The vertical temperature distribution and the layer of minimum temperature." *Journal of Applied Meteorology*, Vol. 2, October, pp. 655-667.

Smith, W.L. (1966). "Note on the relationship between total precipitable water and surface dew point." *Journal of Applied Meteorology*, Vol. 5, October, pp. 726-727.

Smith, W.L. (1968): Reply. *Journal of Applied Meteorology*, Vol. 7, p. 510.